Salt-sensitivity of SigH and Spo0A prevents *Bacillus subtilis* sporulation at high osmolarity avoiding death during cellular differentiation

Nils Widderich[1,¶], Christopher D.A. Rodrigues[2,¶], Fabian M. Commichau[3], Kathleen E. Fischer[1], Fernando H. Ramirez-Guadiana[2], David Z. Rudner[2,*] and Erhard Bremer[1,*]

[1]Department of Biology, Laboratory for Molecular Microbiology, Philipps-University Marburg, Karl-von-Frisch Str. 8, D-35043 Marburg, Germany

[2]Harvard Medical School, Department of Microbiology and Immunobiology, 77 Avenue Louis Pasteur, Boston, MA 02115-5701, USA

[3]Department of General Microbiology, Institute of Microbiology and Genetics, Georg August University Göttingen, Griesebachstr. 8, D-37077 Göttingen, Germany

Running title: High salinity blocks sporulation

Keywords: salt stress – development – sporulation – sigma factors – kinase – cell death

For correspondence during the reviewing and editorial process:

Erhard Bremer: Philipps-University Marburg, Dept. of Biology, Laboratory for Microbiology, Karl-von-Frisch-Str. 8, D-35032 Marburg, Germany. Phone: (+49)-6421-2821529. Fax: (+49)-6421-2828979. E-Mail: bremer@staff.uni-marburg.de

¶These authors contributed equally to this work

*For correspondence. E.B.: E-mail bremer@staff.uni-marburg.de; Tel. (+49)-6421-2821529; (+49)-6421-2828979; D.Z.R.: rudner@hms.harvard.edu; (+1)-617-432-4455; (+1)-617-432-4787

SUPPLEMENTARY MATERIAL

Supplemental Figures

Widderich *et al.*, Figure S1

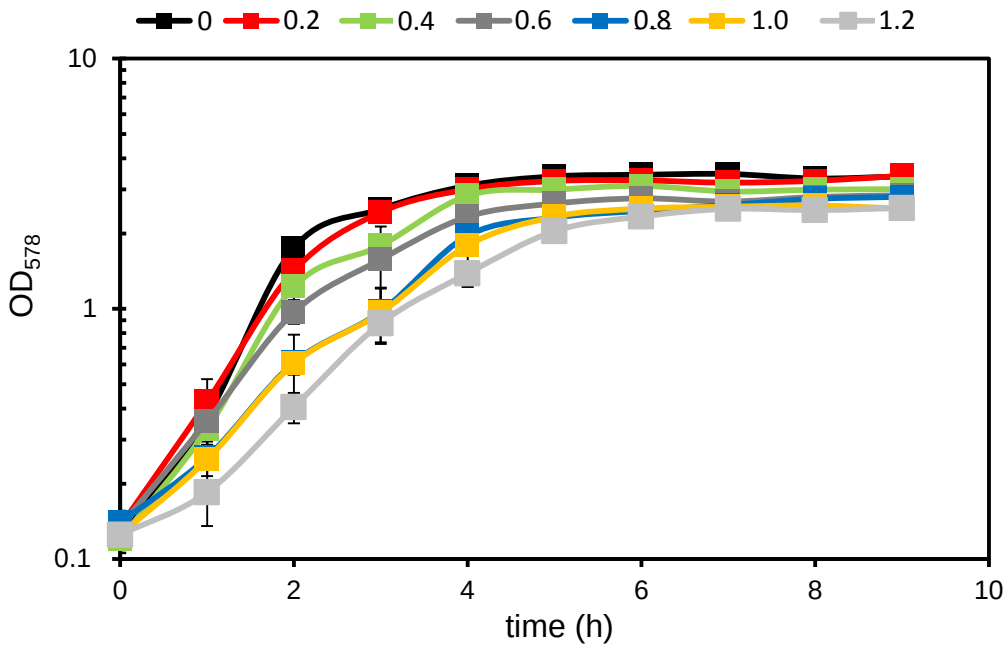

Figure S1. Growth of *Bacillus subtilis* in DSM in the presence of different concentrations of NaCl. Growth curves of *B. subtilis* JH642 cells grown in the presence of the indicated concentrations (in M) of NaCl in nutrient exhaustion medium (DSM). Lag-phase is extended in high salinity-challenged cells (above 0.6 M) but growth rate is only mildly impaired (less than 2-fold at 1.2 M NaCl).

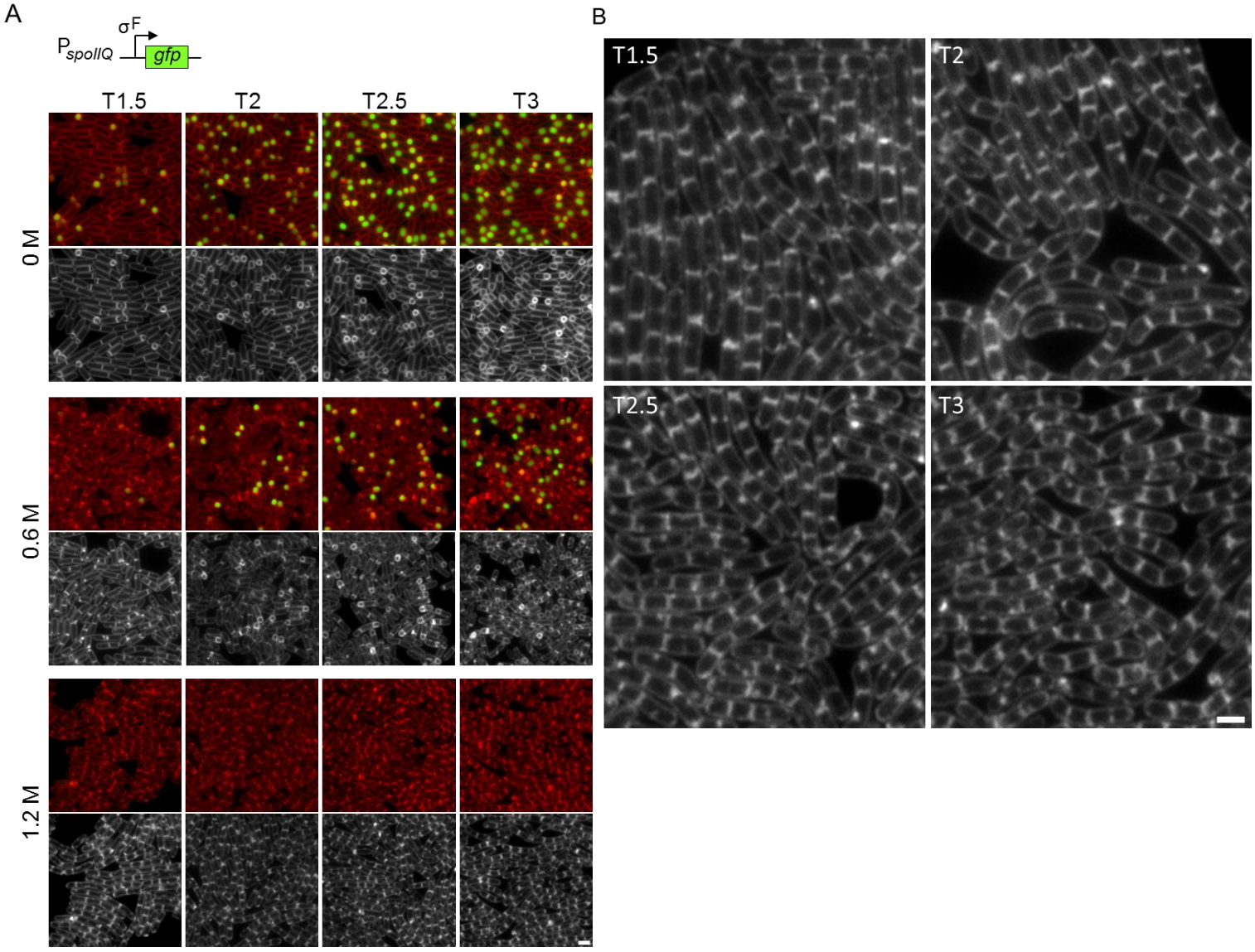

Figure S2. High salinity inhibits sporulation prior to asymmetric cell division. (A) Representative images of cells (strain BDR1048; Table S1) harboring a transcriptional reporter (P_{spoIIQ}-*gfp*) for the forespore-specific transcription factor σ^F induced to sporulate in the indicated concentrations of NaCl. Membranes (false-colored in red) were stained with TMA-DPH and σ^F-dependent expression of the reporter is shown in green. Membranes are also shown in black/white. The time after the initiation of sporulation is indicated. (B) Larger images of the same strain sporulated in the presence of 1.2 M NaCl to highlight the absence of polar septa. For comparison see Figure S9. Scale bar is 2 μm.

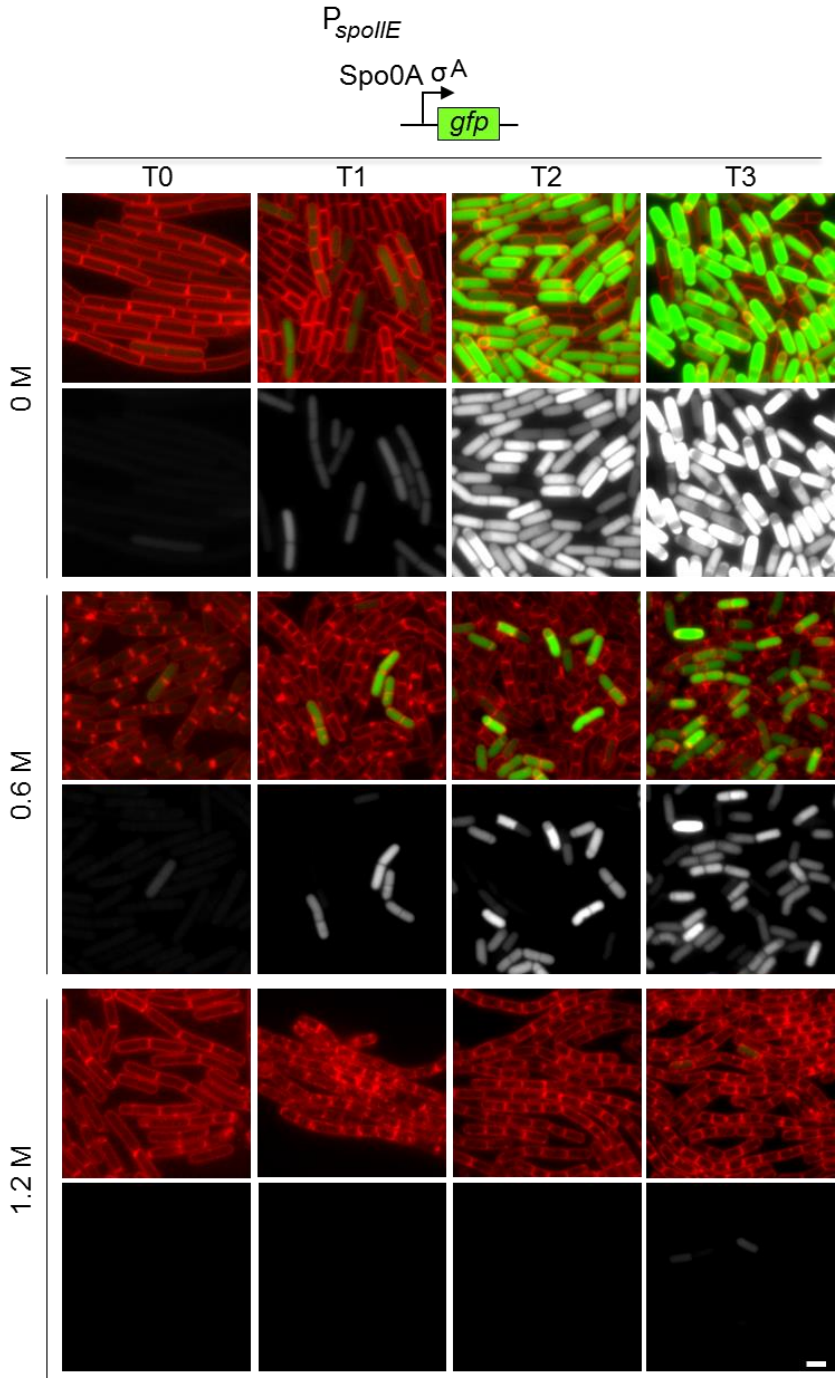

Figure S3. Spo0A activity is impaired in high salt. Representative images of cells (BDR2128) harboring a transcriptional reporter (P_{spoIIE}-*gfp*) for Spo0A activity induced to sporulate in the indicated concentrations of NaCl. For each condition and time point (in hours), GFP fluorescence is shown in black/white and above a merged image of membranes (red) and GFP (green). In the presence of 1.2 M NaCl no cells displayed Spo0A activity, whereas in 0.6 M NaCl a subset of cells displayed Spo0A activity. After polar division, Spo0A activity remains high in the mother cell compartment. All images were scaled identically. The relevant transcription factors that act on the *spoIIE* promoter are indicated above the images. Scale bar indicates 2 μm.

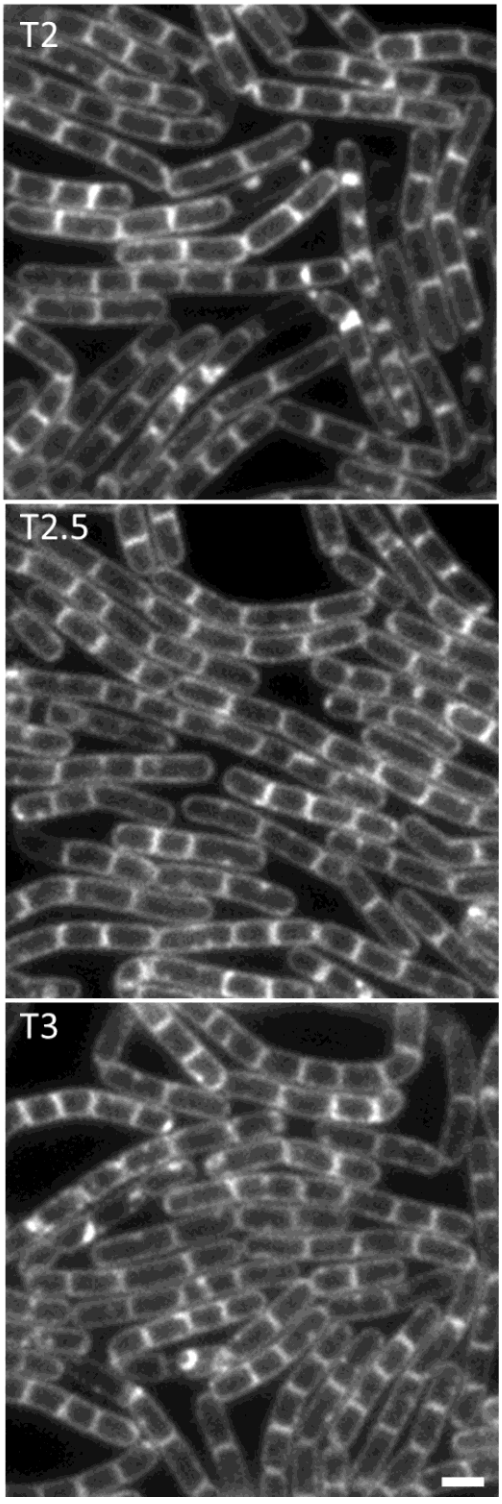

Figure S4. High salinity inhibits sporulation prior to asymmetric cell division. Representative images of cells (strain BDR2128; Table S1) harboring a transcriptional reporter (P_{spoIIE}-*gfp*) to monitor Spo0A-activity induced to sporulate in 1.2M NaCl. The hours after the initiation of sporulation are indicated. Membranes were stained with TMA-DPH and no asymmetric septa were observed at any of the indicated time points. Scale bar indicates 2 μm.

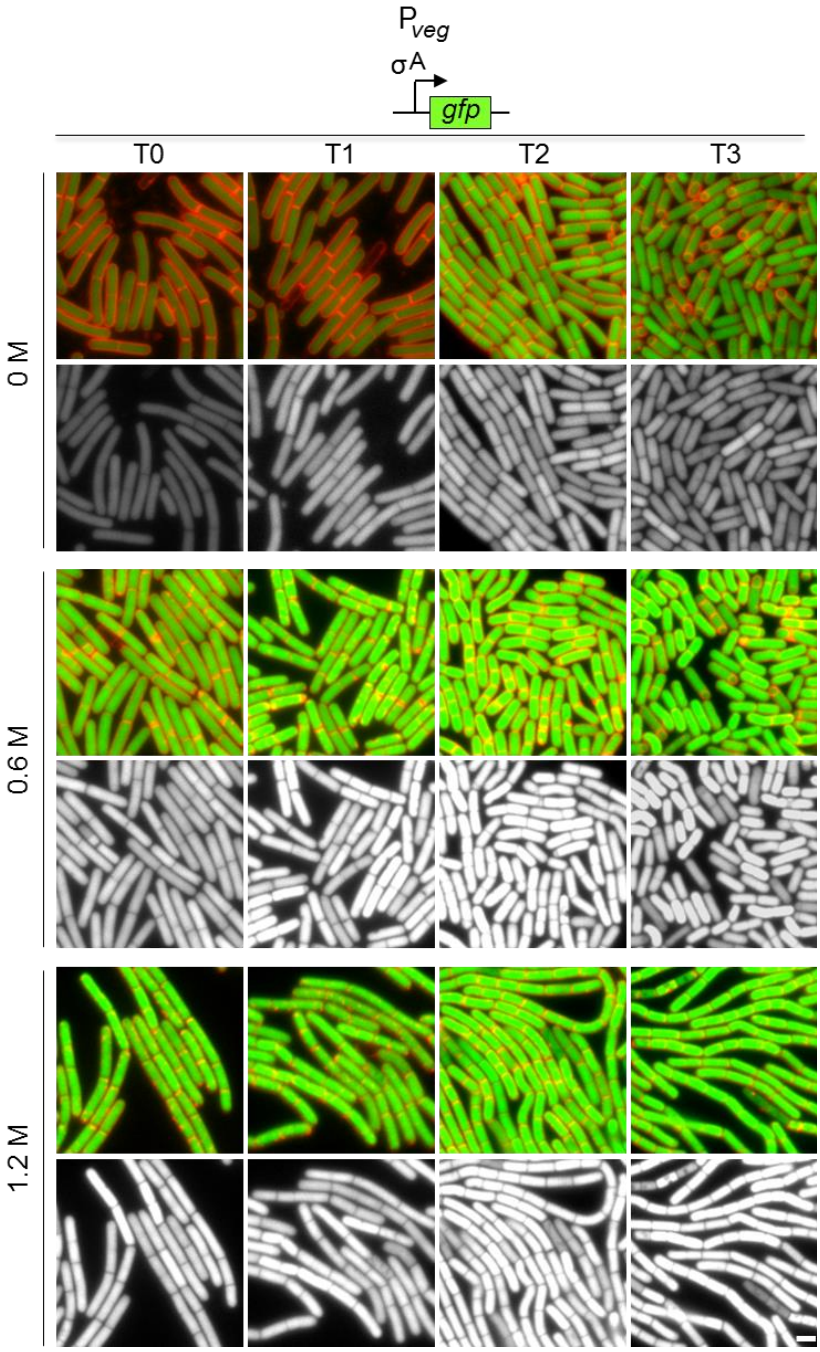

Figure S5. Control for GFP fluorescence and σ^A-dependent gene expression during sporulation in high salt. Representative images of cells (BDR2789) harboring a reporter (P_{veg}-*gfp*) for σ^A-dependent transcription induced to sporulate in the indicated concentrations of NaCl. For each condition and time point (in hours), GFP fluorescence is shown in black/white below a merged image of membranes (red) and GFP (green). GFP produced under σ^A control was easily detectable in 0.6M and 1.2M NaCl indicating that GFP fluorescence is not inhibited by high salt. Interestingly, σ^A-directed gene expression was higher in the presence of salt than in its absence, perhaps due to the absence of sigma factor competition. Scale bar indicates 2 μm.

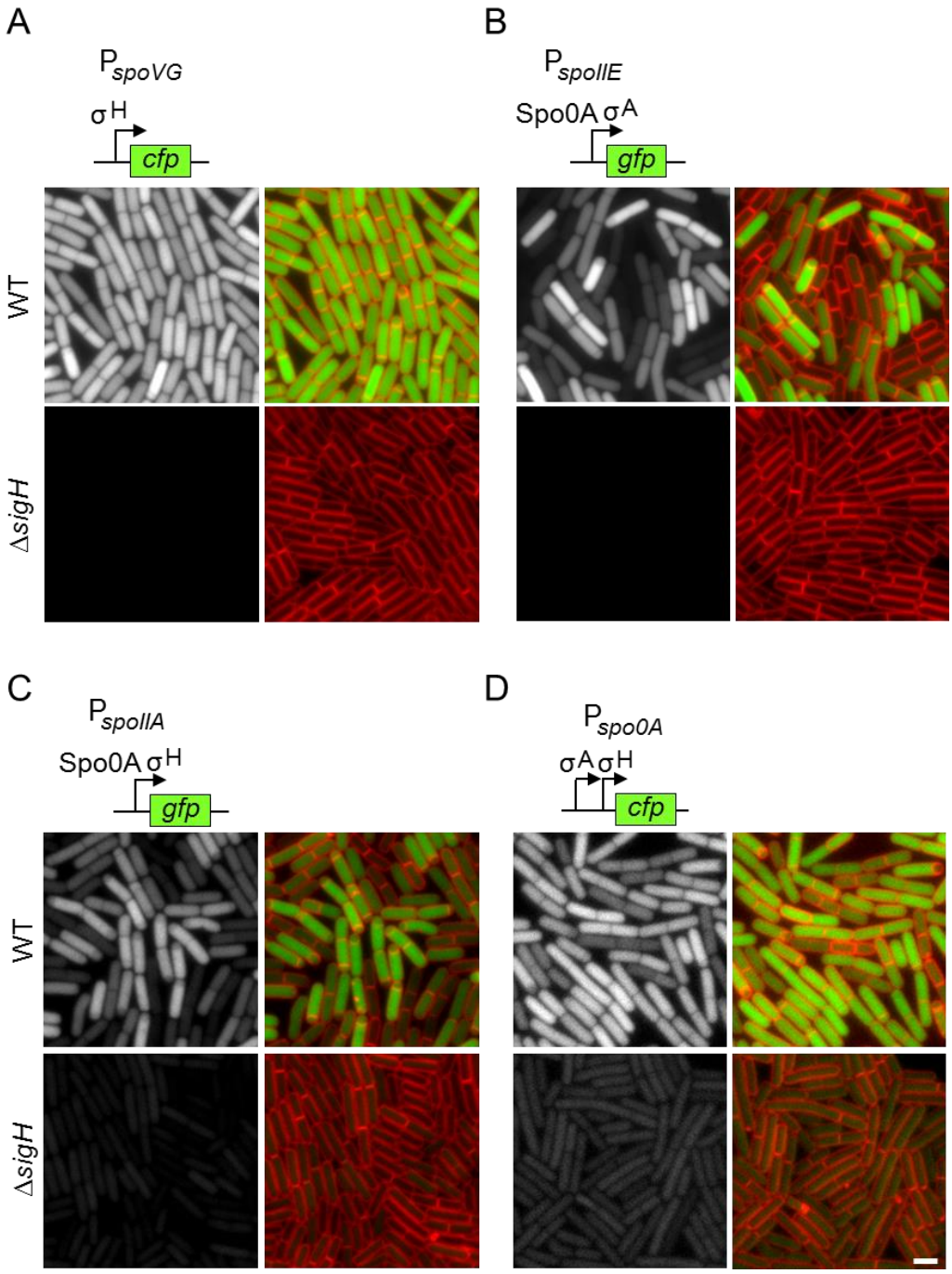

Figure S6. σ^H dependence of the transcriptional reporters used in this study. Representative images of sporulating cells at hour 1.5 harboring the indicated fluorescent reporters in wild-type and in cells lacking the gene (*sigH*) encoding σ^H. (A) The P_{spoVG}-*cfp* reporter in WT (top, BDR3064) and the *sigH* null (bottom, BDR3065), (B) the P_{spoIIE}-*gfp* reporter in WT (top, BDR2128) and the *sigH* null (bottom, BDR3074), (C) the P_{spoIIA}-*cfp* reporter in WT (top, BDR1799) and the *sigH* null (bottom, BDR3056) and (D) the P_{spo0A}-*cfp* reporter in WT (top, BDR3080) and the *sigH* null (bottom, BDR3083). Images are GFP/CFP-dependent fluorescence (black/white) and overlays of GFP/CFP (green) with membrane (red). Scale bar indicates 2 μm.

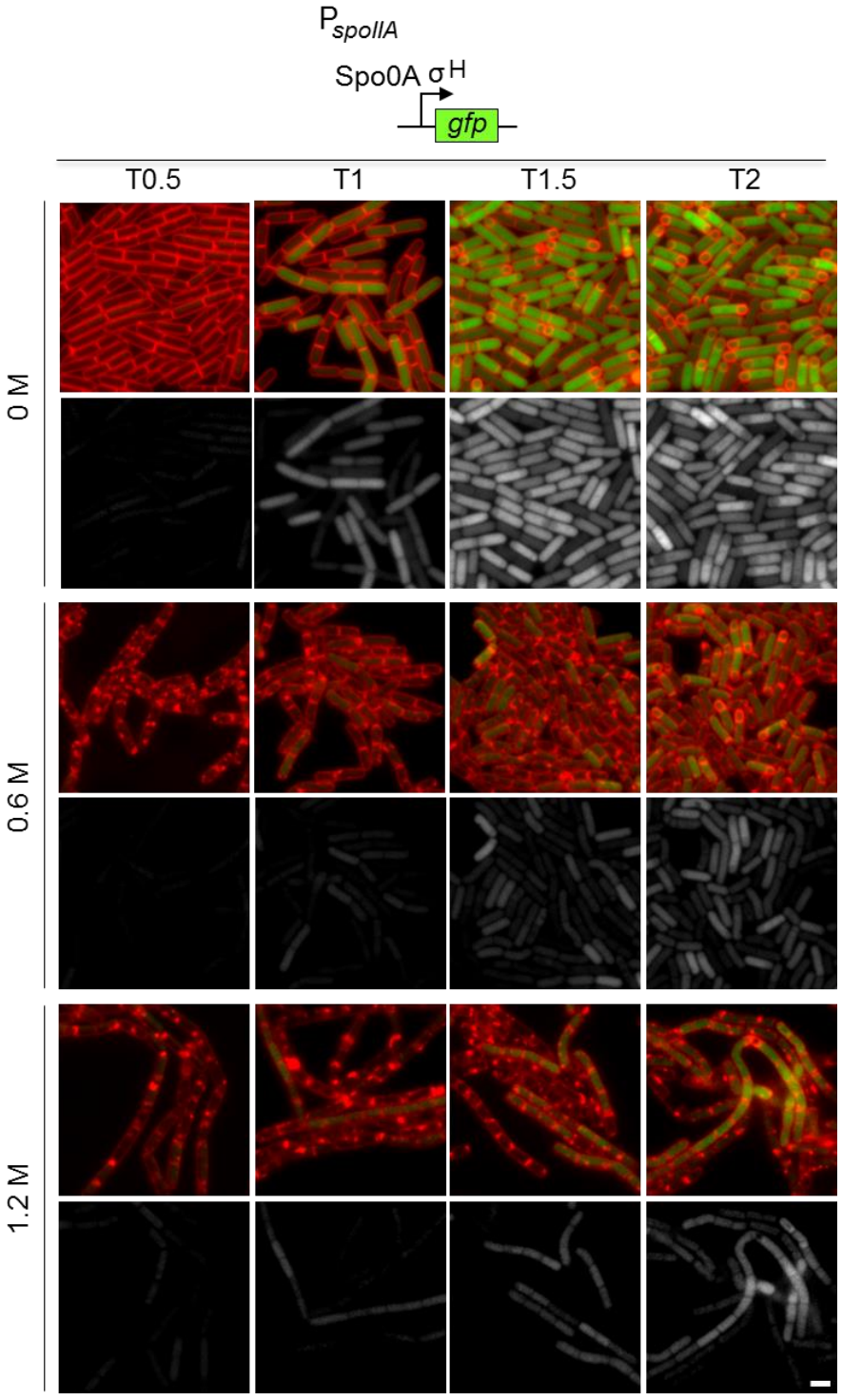

Figure S7. Transcription from the P_{spoIIA} promoter is reduced in the presence of high-salt. Representative images of cells (BDR1799) harboring a transcriptional reporter (P_{spoIIA}-*gfp*) for Spo0A- and σ^H-dependent activity induced to sporulate in the indicated concentrations of NaCl. For each condition and time point (in hours), GFP fluorescence is shown in black/white below a merged image of membranes (red) and GFP (green). Transcription from this promoter is reduced in 0.6 M NaCl and 1.2M NaCl. All images were scaled identically. The relevant transcription factors that act on the *spoIIA* promoter are indicated at the top. Scale bar indicates 2 μm.

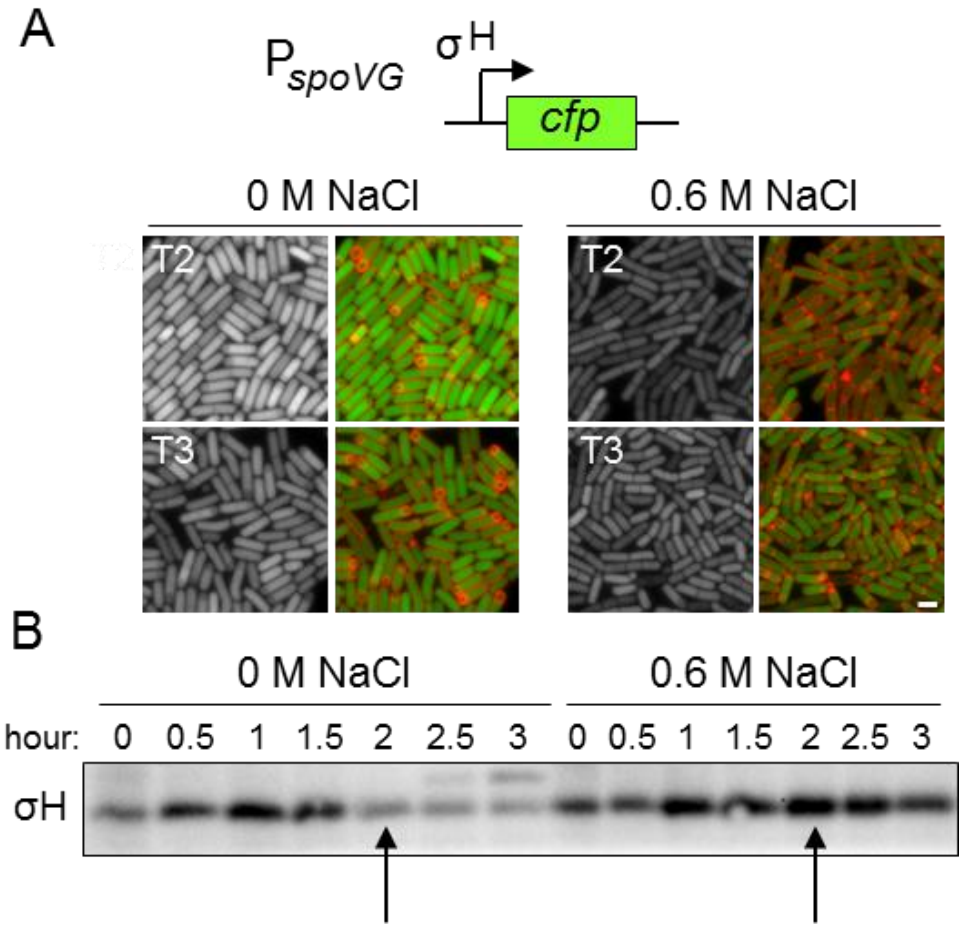

Figure S8. Comparison of σ^H activity and σ^H protein level in the presence and absence of 0.6 M NaCl. (A) Representative images of cells (strain BDR3064) harboring a transcriptional reporter (P_{spoVG}-*cfp*) for σ^H-dependent activity induced to sporulate in the indicated concentrations of NaCl and imaged at hours 2 (T2) and 3 (T3) after the onset of sporulation. All images were scaled identically. Scale bar indicates 2 μm. (B) Immunoblot analysis assessing σ^H levels in wild-type (strain PY79) induced to sporulate in the presence of the indicated concentrations of NaCl. Black arrows point to σ^H levels at the relevant time point for comparison to the images in (A). Although σ^H levels are higher in the 0.6 M NaCl condition, transcription from the σ^H-dependent promoter is lower.

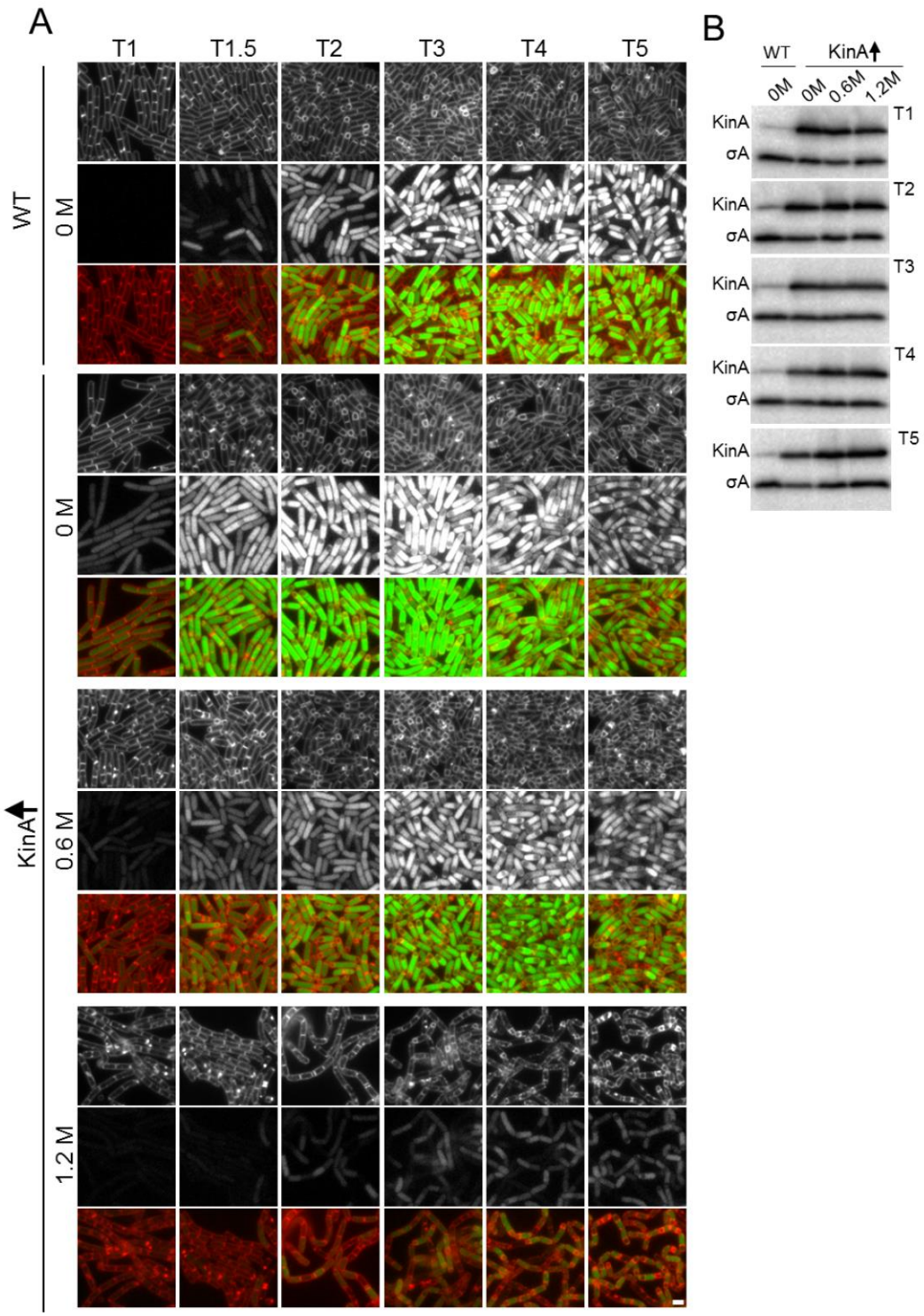

Figure S9. Overexpression of *kinA* bypasses the early salt-sensitive block in sporulation. (A) Representative images of cells harboring the Spo0A activity reporter (P_{spoIIE}-*gfp*) induced to sporulate in the presence of the indicated concentrations of NaCl. Images are from the wild-type (strain BDR2128) and a strain (BDR3087) harboring an IPTG-inducible allele of *kinA*. The time (in hours) after the initiation of sporulation is indicated. Membranes and GFP are shown in black/white with a merged image below. Scale bar indicates 2 μm. (B) Immunoblot analysis assessing the levels of KinA in the same strains in the indicated concentrations of NaCl. σ^A serves as a loading control.

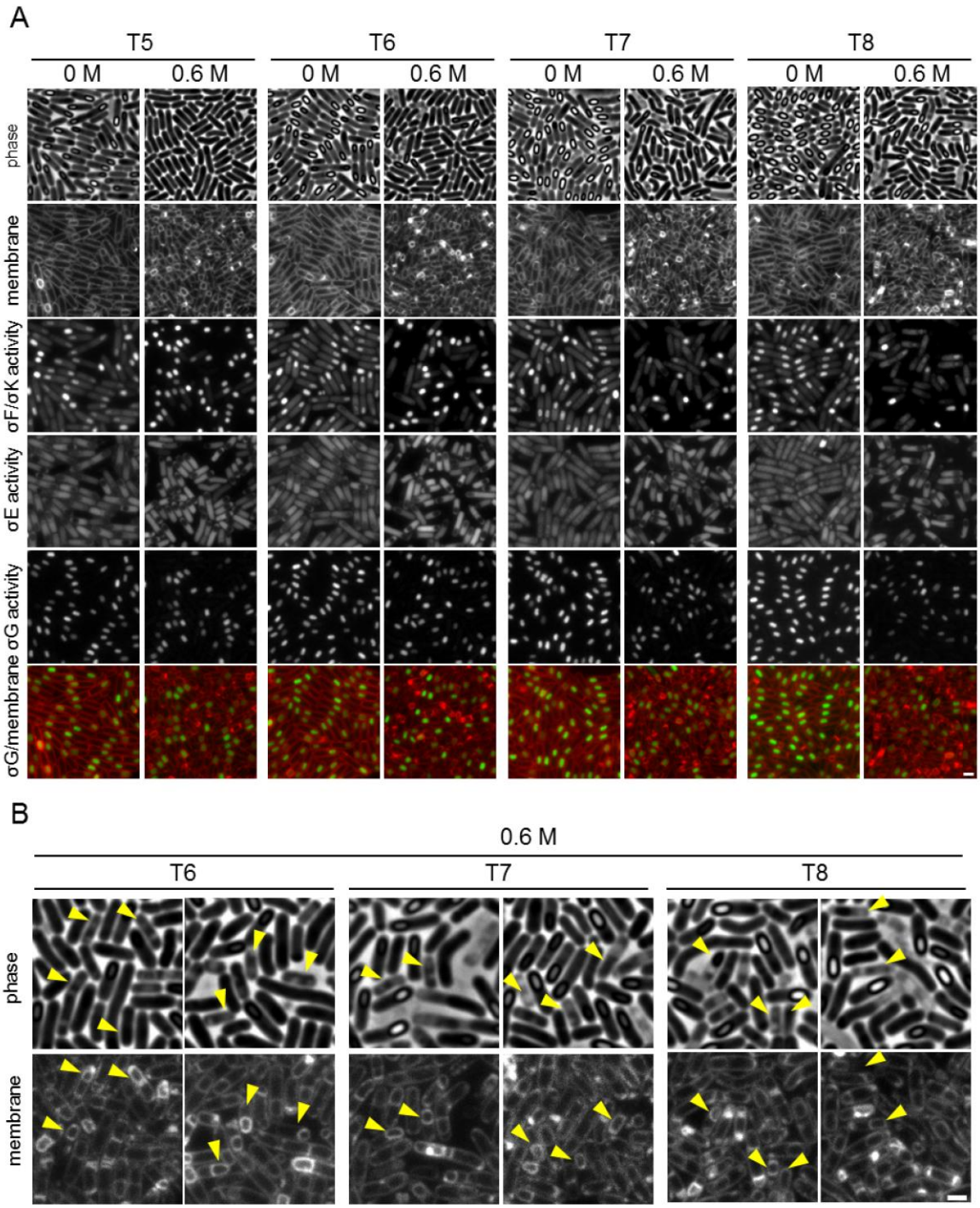

Figure S10. High salinity impairs engulfment, late forespore gene expression, reduces the production of phase bright spores and causes lysis. (A) Representative images of the *kinA* overexpression strain (BCR1274) harboring transcriptional reporters for all four stage- and compartment-specific sigma factors induced to sporulate in the presence of the indicated concentrations of NaCl (see main text for strain details). The time (in hours) after the initiation of sporulation is indicated. Phase panels highlight the reduction in phase bright spores and the increased lysis in cells sporulated in 0.6 M NaCl. (B) Representative images of the *kinA* overexpression strain highlighting the lysis of sporulating cells at the indicated time points. Yellow arrowheads point to sporulating cells that have lysed or are on the verge of lysing. Scale bar indicates 2 μm.

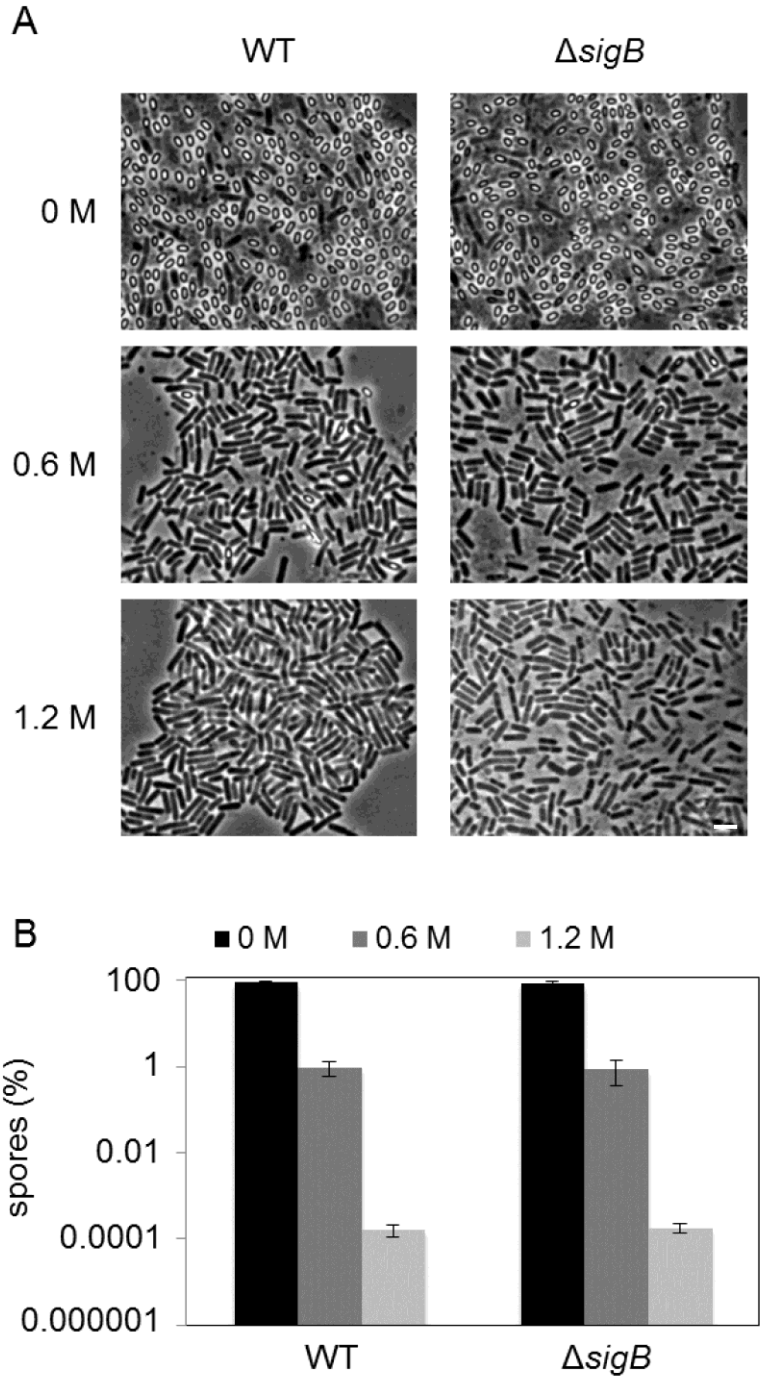

Figure S11. Sporulation at high salinity in a *sigB* null strain is similar to wild type. (A) Representative phase-contrast images of wild-type (WT; JH642) and a *sigB* null mutant (FSB5) sporulated by nutrient exhaustion in the presence of the indicated concentrations of NaCl. Scale bar indicates 4 μm. (B) The bar graph shows the negative effects of high salinity on sporulation.

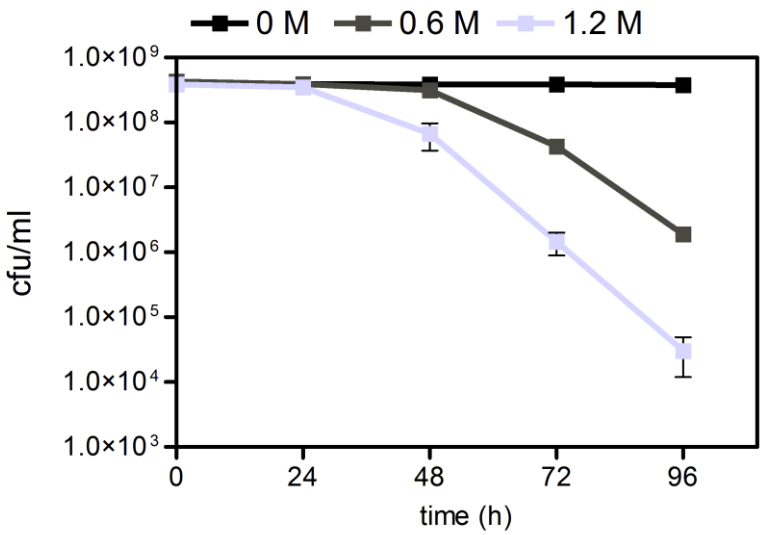

Figure S12. Survival of *Bacillus subtilis* cells grown in the presence of different concentrations of NaCl. The colony forming units per ml (cfu/ml) of *B. subtilis* JH642 cells incubated for the indicated times (in hours) in nutrient exhaustion medium (DSM) in presence of 0 M, 0.6 M or 1.2 M NaCl. In the presence of 0 M NaCl, the cells form dormant spores and the colony forming units remain constant over 96 hours. Cells grown in medium with high salt lose viability after 48-72 hours.

Table S1. Strains used in this study

strain	genotype	source
JH642	*trpC2 pheA1*	(Dean *et al*., 1977)
168	*trpC2*	(Burkholder and Giles, 1947)
3610	undomesticated wild type (biofilm strain)	(Branda *et al*., 2001)
DK1042	comI^{Q12L}	(Konkol *et al*., 2013)
PY79	Prototrophic wild-type strain	(Youngman *et al.*, 1983)
B. mojavensis	wild-type strain	(Earl *et al*., 2012)
FSB5	*sigBD2::spc*	(Spiegelhalter and Bremer, 1998)
BDR1753	*sigH::kan, trpC2, pheA1*	D. Rudner
BDR1048	*amyE::PspoIIQ-gfp (spec)*	D. Rudner
BDR2128	*amyE::PspoIIE-gfp (spec)*	(Fujita and Losick, 2003)
BDR2331	*kinAΩPhyper-spank-kinA(spec)*	(Fujita and Losick, 2005)
BDR2789	*sacA::Pveg-gfp (phleo)*	D. Rudner
BDR485	*rpoCΩpETΔrpoC (rpoC-his6) (neo)*	(Fujita and Sadaie, 1998)
BCR1071	*yycR::PsspB-rbsopt-cfp (phleo), amyE::PspoIID-mCherry(spec), pelB::PspoIIQ-yfp (kan), lacA::PgerE-yfp (tet)*	(Meeske *et al., in press*)
BCR1274	*yycR::PsspB-rbsopt-cfp (phleo), amyE::PspoIID-mCherry(Bsub OPT)(spec), pelB::PspoIIQ-yfp (kan), lacA::PgerE-yfp (tet), kinAΩPhyperspank-kinA (cat)*	this study
BDR1799	*amyE::PspoIIA-gfp (cat)*	D. Rudner
BDR3056	*sigHΔ, amyE::PspoIIA-gfp cat*	this study
BDR3064	*amyE::PspoVG-cfp (spec)*	this study
BDR3065	*sigH::kan, amyE::PspoVG-cfp (spec)*	this study
BDR3074	*sigH::kan, amyE::PspoIIE-gfp (spec)*	this study
BDR3080	*amyE::Pspo0A-cfp (spec)*	this study
BDR3083	*sigH::kan, amyE::Pspo0A-cfp (spec)*	this study
BDR3087	*kinAΩPhyper-spank-kinA(cat), amyE::PspoIIE-gfp (spec)*	this study
BDR3090	*amyE::PsigH-cfp (spec)*	this study
BDR3095	*sigH::kan, amyE::PsigH-cfp (spec)*	this study
NWB6	JH642-derived suppressor allowing increased sporulation at high salinity	this study
NWB7	JH642-derived suppressor allowing increased sporulation at high salinity	this study
NWB11	JH642-derived suppressor allowing increased sporulation at high salinity	this study
NWB13	JH642-derived suppressor allowing increased sporulation at high salinity	this study
NWB16	JH642-derived suppressor allowing increased sporulation at high salinity	this study
NWB17	JH642-derived suppressor allowing increased sporulation at high salinity	this study
NWB19	JH642-derived suppressor allowing increased sporulation at high salinity	this study
NWB21	JH642-derived suppressor allowing increased sporulation at high salinity	this study
NWB22	JH642-derived suppressor allowing increased sporulation at high salinity	this study
NWB24	JH642-derived suppressor allowing increased sporulation at high salinity	this study
NWB25	JH642-derived suppressor allowing increased sporulation at high salinity	this study

Table S2. Plasmids used in this study

plasmids	description	source
pKM161	*amyE::P$_{spoIIQ}$-cfp XhoI (spec) (amp)*	D. Rudner
pNW1	*amyE::P$_{sigH}$-cfp (spec) (amp)*	this study
pNW2	*amyE::P$_{spoVG}$-cfp (spec) (amp)*	this study
pNW4	*amyE::P$_{spo0A}$-cfp (spec) (amp)*	this study

Table S3. Oligonucleotide primers used in this study

primer	sequence
oDR1200	ccatagtagttcctccttatgtaagctttttccctatataaaagcattagtgtatc
oDR1202	tcgccattcgccagggctgcaggaattcgaaataataagaaaagtgattctggg
oDR1203	ttattgccaaaagagctatccacgc
oDR1204	aacaacggcgtttaagccgttgttt
oDR1205	attttcggacaggggcattgcgga
oDR1206	actgtcaatatagcataaattccta
oDR1207	tattttgatccctcttcacttctcag
oDR1208	taatgaccacttaataagctcatgt
oDR75	ataacatgtattcacgaacg
oDR1217	cgcgaattcttatggaaaagaaaaagcaagctgactgccgg
oDR1218	cgcaagcttaattttctccacgtttcttcctcccc
oDR1219	gcgaagcttatggtttcaaaaggcgaagaactg
oDR1220	cgcggatcctagcatgcatgctagcat
oDR1221	cgcgaattcagagaggtagaaacgattgaaaggcg
oDR1222	cgcaagcttctgtagattcactccgatcccc
oML79	ctcttgccagtcacgttacg
oDR77	ggcagacatggcctgcccgg

Supplementary methods

Strain construction

All *B. subtilis* strains were constructed by standard transformation with genomic DNA or linearized plasmids followed by selection on LB agar plates supplemented with appropriate antibiotics.

Plasmid construction

pNW1 [amyE::P_{sigH}-*cfp* (spec)] was obtained by amplification of P_{sigH} from genomic DNA of strain PY79 using primers oDR1221 and oDR1222 (Table S3) and by amplification of *cfp* from plasmid pKM161 (Table S2) using oligonucleotides oDR1219 and oDR1220 (Table S3). The P_{sigH} product was restricted with EcoRI and HindIII, the *cfp* product with HindIII and BamHI and the pKM161 plasmid with EcoRI and BamHI. Restricted products and backbone of plasmid pKM161 were purified from agarose gels and then ligated in a three-way ligation using T4 DNA Ligase. The resulting plasmid was transformed into *E. coli* DH5α and plated on LB agar plates containing ampicillin (100 μg ml^{-1}). DNA sequencing with primers oML79 & oDR77 (Table S3) was performed to confirm the structure of the desired P_{sigH}-*cfp* reporter plasmid (Table S2).

pNW2 [amyE::P_{spoVG}-*cfp* (spec)] was obtained by isothermal assembly (Gibson, 2011). The isothermal assembly reaction contained two PCR products: (i) P_{spoVG} (amplified from genomic DNA of strain PY79 using primers oDR1200 and oDR1202; Table S3), and (ii) plasmid pKM161 that was restricted with EcoRI-HF and HindIII-HF. The resulting plasmid was transformed into *E. coli* DH5α and plated on LB agar plates containing ampicillin. Sequencing with primer oDR75 (Table S3) was performed to confirm the structure of the desired P_{spoVG}-*cfp* reporter construct (Table S2).

pNW4 [amyE::P_{spoOA}-*cfp* (spec)] was obtained by amplification of P_{spo0A} from chromosomal DNA of strain PY79 using primers oDR1217 and oDR1218 (Table S3) and by amplification of *cfp* from plasmid pKM161 (Table S2) using oligonucleotides oDR1219 and oDR1220 (Table S3). The resulting P_{spo0A} product was restricted with EcoRI and HindIII, the *cfp* product with HindIII and BamHI and plasmid pKM161 with EcoRI and BamHI. Restricted products and backbone of pKM161 were purified from agarose gels and combined in a three-way ligation using T4 DNA Ligase. The resulting plasmid was transformed into *E. coli* DH5α and plated on LB agar plates containing ampicillin. Sequencing with primers oML79 & oDR77 (Table S3) was performed to confirm the structure of the desired P_{spo0A}-*cfp* reporter construct (Table S2).

References

Branda, S.S., Gonzalez-Pastor, J.E., Ben-Yehuda, S., Losick, R., and Kolter, R. (2001) Fruiting body formation by *Bacillus subtilis*. *Proc Natl Acad Sci U S A* **98**: 11621-11626.

Burkholder, P.R., and Giles, N.H., Jr. (1947) Induced biochemical mutations in *Bacillus subtilis*. *Am J Bot* **34**: 345-348.

Dean, D.R., Hoch, J.A., and Aronson, A.I. (1977) Alteration of the *Bacillus subtilis* glutamine synthetase results in overproduction of the enzyme. *J Bacteriol* **131**: 981-987.

Earl, A.M., Eppinger, M., Fricke, W.F., Rosovitz, M.J., Rasko, D.A., Daugherty, S., Losick, R., Kolter, R., and Ravel, J. (2012) Whole-genome sequences of *Bacillus subtilis* and close relatives. *J Bacteriol* **194**: 2378-2379.

Fujita, M., and Losick, R. (2003) The master regulator for entry into sporulation in *Bacillus subtilis* becomes a cell-specific transcription factor after asymmetric division. *Genes & Development* **17**: 1166-1174.

Fujita, M., and Losick, R. (2005) Evidence that entry into sporulation in *Bacillus subtilis* is governed by a gradual increase in the level and activity of the master regulator Spo0A. *Genes & Development* **19**: 2236-2244.

Fujita, M., and Sadaie, Y. (1998) Rapid isolation of RNA polymerase from sporulating cells of *Bacillus subtilis*. *Gene* **221**: 185-190.

Gibson, D.G. (2011) Enzymatic assembly of overlapping DNA fragments. *Methods Enzymol* **498**: 349-361.

Konkol, M.A., Blair, K.M., and Kearns, D.B. (2013) Plasmid-encoded ComI inhibits competence in the ancestral 3610 strain of *Bacillus subtilis*. *J Bacteriol* **195**: 4085-4093.

Meeske, A.J., Rodrigues, C.D.A., Brady, J., Lim, H.C., Bernhardt, T.G., and Rudner, D.Z. (2015) High throughput genetic screens identify a large and diverse collection of new sporulation genes in *Bacillus subtilis*. PLoS Biology, *in press*.

Spiegelhalter, F., and Bremer, E. (1998) Osmoregulation of the *opuE* proline transport gene from *Bacillus subtilis*: contributions of the sigma A- and sigma B-dependent stress-responsive promoters. *Molecular Microbiology* **29**: 285-296.

Youngman, P.J., Perkins, J.B., and Losick, R. (1983) Genetic transposition and insertional mutagenesis in *Bacillus subtilis* with *Streptococcus faecalis* transposon Tn917. *Proc Natl Acad Sci U S A* **80**: 2305-2309.